



NMR Spectroscopy:

From 60-MHz instruments to the upcoming 900-MHz systems that run multi dimensional experiments, NMR has proven to be one of chemistry's most important tools.

The detection of nuclear magnetic resonance (NMR) in condensed phases was first reported in the middle of the 20th century by physicists attempting to measure nuclear magnetic moments more accurately. Soon after, it was found that the resonance frequency depends not only on the atomic nucleus but also on its chemical environment. This discovery of the chemical shift caught the attention of chemists, who recognized the potential of NMR for determining the structures of molecules.

Today, NMR is applied in ways that could not have been imagined when the first measurements were made. Not only has NMR become one of the most powerful methods for determining molecular structures, it has found many applications in chemistry and other fields, such as materials science, medicine, and biology. This retrospective reviews the development of instrumentation and methodology for chemical applications of NMR spectroscopy.

Past and Present

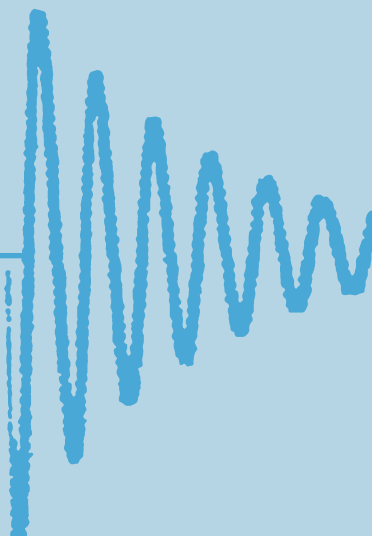
The discovery

To account for hyperfine splittings in the optical spectra of certain atoms, Pauli, in 1924, proposed that their nuclei possess spin angular momentum and thus have magnetic moments (*1*). During the same period, Gerlach and Stern reported direct verification of nuclear magnetic moments in atomic beam experiments (*2*). In 1938, Rabi and colleagues first observed the resonance effect by applying electromagnetic radiation in beam experiments (*3*). After unsuccessful attempts by several labs to observe NMR in condensed phases, research groups led by Bloch at Stanford and Purcell at Harvard reported in 1946 the observation of ^1H NMR in liquid water and solid paraffin wax (*4, 5*), for which they shared the 1953 Nobel Prize in Physics.

Early applications of NMR focused on the measurement of nuclear magnetic moments on the basis of the assumption that the resonance frequency (ν) of a nucleus depends only on its magnetogyric ratio (γ) and the applied magnetic field (\mathbf{B}_0), according to the Larmor equation $\nu = \gamma \mathbf{B}_0 / 2\pi$. However, in 1950, Proctor and Yu unexpectedly observed two ^{14}N resonance frequencies for NH_4NO_3 (*6*). By accident, they had discovered the chemical shift. About the same time, Dickinson noticed similar effects for ^{19}F in several compounds, and Arnold, Dharmatti, and Packard observed separate resonances for the $-\text{CH}_3$, $-\text{CH}_2-$, and $-\text{OH}$ protons of ethanol (Figure 1) (*7, 8*). Arnold and colleagues also observed that the relative intensities of the resonances were the same as the relative numbers of protons. Following these reports, Gutowsky and others began systematic studies to correlate chemical shifts with molecular structure (*9*).

During this same period, spin-spin coupling through chemical bonds was discovered. It was already known that direct through-space, or dipolar, interactions between nuclear magnetic moments broadened and split NMR spectra of solids, but these dipole-dipole interactions vanish in a liquid when the internu-

Dallas L. Rabenstein
University of California–Riverside



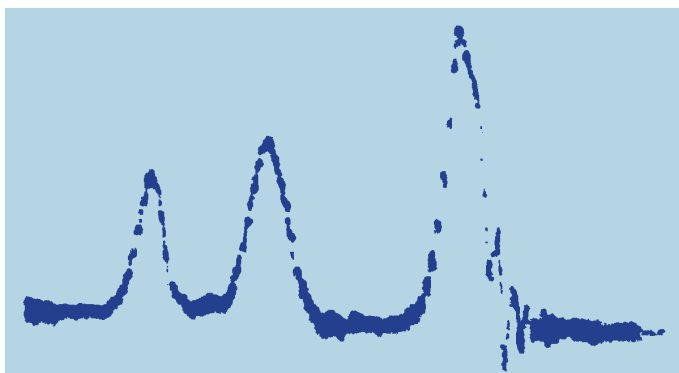


FIGURE 1. 32.4-MHz ^1H NMR spectrum of ethanol as first observed in 1951.

The peaks from left to right are for the $-\text{OH}$, $-\text{CH}_2$, and $-\text{CH}_3$ protons (δ).

clear vector is moving rapidly and randomly. The observation of multiplets for neighboring groups of nuclei in NMR spectra of liquids required a different mechanism to account for interactions between their nuclear magnetic moments (10–12). Purcell and Ramsey provided the explanation in terms of the indirect through-bond, or scalar, spin–spin coupling mechanism (13).

Within seven years of the first observation of NMR in condensed phases, the chemical shift, the dependence of resonance intensity on concentration, spin–spin coupling, nuclear spin relaxation, the effect of chemical exchange on NMR spectra, and the nuclear Overhauser (NOE) effect had all been described. The stage was set for chemists to apply NMR.

Instrumentation in the early days

The availability of commercial instruments played a major role in the rapid development of NMR. Within six years of the first report of NMR in condensed phases, Varian Associates delivered a commercial NMR spectrometer, the HR-30. This continuous wave (cw) instrument was based on a 7050-G (0.7-T) electromagnet. (The resonance condition for cw is achieved either by sweeping the magnetic field while holding the radio frequency constant or vice versa.) The HR-30 had a ^1H resonance frequency of 30 MHz. Sensitivity was so low that only neat liquids or concentrated solutions gave detectable signals, and, according to Jim Shoolery, manager of the Varian NMR applications lab, the instrument was an operator's nightmare (14).

To improve sensitivity and increase chemical shift dispersion, commercial instrument development focused on increasing the magnetic field strength. The HR-30 was followed by several instruments in this series, including the HR-100 (100 MHz ^1H) and, in 1964, the HR-220 (220 MHz ^1H), which was based on a 5.17-T superconducting magnet. However, it was the Varian A-60 that brought routine NMR to chemists.

The A-60, a 60-MHz proton-only cw instrument based on a 1.4-T electromagnet, was introduced to the analytical community at the 1961 Pittsburgh Conference. With the A-60's user-friendly operation, magnetic field stability provided by its field/frequency lock, and flatbed recorder for producing spectra on precalibrated chart paper, NMR quickly became the chemist's method of choice for following the progress of synthesis and analyzing the structures of synthetic and natural products (14). Other innovations during these years included the use of sample spinning and field gradient shims to improve resolution and the development of homonuclear spin decoupling to aid spectral assignment.

Although NMR rapidly became an indispensable tool for chemists, its range of applications was limited to only a few of the many NMR-active nuclei because of the technique's intrinsically low sensitivity. Most cw NMR experiments were done on nuclides with a spin quantum number (I) of $1/2$, a high natural abundance, and a large γ . ^1H was the most studied nucleus, followed by ^{19}F and ^{31}P , both of which are 100% naturally abundant.

To improve sensitivity, signal averaging with a computer of average transients (CAT) was introduced in 1964. With the CAT, the spectrum was digitized and stored in 1024 channels as it was scanned. The process was then repeated, with the next digitized spectrum added to that already stored in the CAT. Signals increase in proportion to the number of scans (n) that are co-added, while noise increases in proportion to $n^{1/2}$, giving an $n^{1/2}$ increase in S/N. However, the amount of sensitivity enhancement that could be achieved by signal averaging with the CAT was limited because the spectrum had to be scanned slowly to avoid line shape distortions. Nevertheless, with overnight runs, detection limits for ^1H NMR could be lowered ~ 10 -fold, and, by using spectra for relatively concentrated solutions, it was possible to measure other NMR-active nuclei, including ^{13}C . Broadband ^1H decoupling was developed at about this time to collapse ^{13}C multiplets to singlets, with the added benefit that resonance intensity can be further increased by up to 200% by NOE.

It was the Varian A-60 that brought routine NMR to chemists.

The Fourier transform revolution

Most NMR spectra were measured by the cw method during the first 25 years of NMR. Today, virtually all NMR spectrometers operate in the pulse/FT mode.

It is convenient to describe the FT-NMR experiment using

a classical vector model in which the individual nuclear magnetic moments are considered to be precessing around \mathbf{B}_0 with no phase coherence. Because the lower energy state is slightly more populated, there is a net macroscopic magnetization in the direction of \mathbf{B}_0 , which is taken to be along the z axis (Figure 2). The pulse/FT spectrometer detects a nuclear induction signal from macroscopic magnetization in the transverse (xy) plane, M_{xy} . At equilibrium, M_{xy} is zero. In FT-NMR, a short rf pulse perturbs the magnetization and creates a nonzero M_{xy} , which precesses around the z axis at the Larmor frequency. The precessing M_{xy} induces a transient signal, the free induction decay (FID), in a receiver coil orthogonal to the direction of \mathbf{B}_0 . Because the rf pulse excites nuclei over a wide frequency range, the FID is a composite of the time domain signals from all the nuclei with resonances in that frequency range. The FID is Fourier transformed to give the frequency domain spectrum.

Although the first high-resolution FT-NMR spectrum was not reported until 1966 (15), pulse methods were actually used in some of the earliest NMR experiments. In 1950, Hahn reported the spin-echo pulse method for determining relaxation times (16). However, applications of the pulse method were limited because spectral information had to be extracted directly from the FID, which for more than a couple of resonances is quite complicated.

In 1956, Lowe and Norberg pointed out that the time domain FID and the frequency domain spectrum form an FT pair. The first high-resolution FT-NMR spectrum was by Ernst and Anderson, who were investigating FT-NMR as a multichannel method to increase sensitivity (15). Sensitivity enhancement by signal averaging in cw NMR is inefficient because the spectrum is scanned one resolution element at a time, whereas the FID contains all the spectral information for a given nuclide. Thus, signal averaging to increase sensitivity is much more efficient in the time domain. For example, a typical scan in cw NMR might take as long as 500 s compared with a typical time of 2–3 s for the acquisition of a FID in FT-NMR.

Because there were no laboratory computers in 1965, the FID was digitized and stored in a CAT. It is interesting to look back at how the FT part of the first pulse/FT NMR experiments was done.

“When Ernst and Anderson started this research, there were no small laboratory computers available, and data storage and retrieval methods were very crude. The experimental FID, digitized initially on the CAT, had to be converted into punched paper tape and then transcribed onto IBM punch cards (one data point per card). These cards were then taken to an adjacent building where the IBM 7090 computer was housed, for FT processing overnight, competing (mostly unsuccessfully) with the rival demands of Varian Associates payroll and factory inventory processing. If the spectrum needed to be rephased—and it almost always did—another day would be wasted before the new spectrum was obtained.” (17)

Fortunately, small laboratory computers that could be dedicated to an NMR spectrometer became available about this

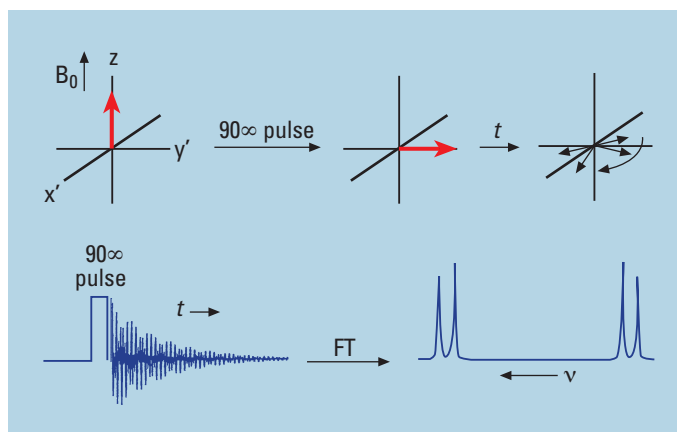


FIGURE 2. Classical vector description of the pulse/FT NMR experiment.

The ensemble of nuclear magnetic moments gives rise to a net macroscopic magnetization, which is aligned with \mathbf{B}_0 , the externally applied magnetic field. The macroscopic magnetization is perturbed by an rf pulse to create transverse magnetization (M_{xy}), which then precesses at the Larmor frequencies of the nuclear magnetic moments excited by the rf pulse. In this example, the rf pulse is a 90° pulse (i.e., it rotates the macroscopic magnetization through 90° into the transverse plane). The precessing transverse magnetization generates a nuclear induction signal, the FID, which is detected as a function of time. In this example, the FID contains four frequencies; Fourier transformation gives the frequency domain spectrum.

time. Also, Cooley and Tukey reported that the FT algorithm could be made more efficient by restricting the size of the data set to 2^n points, where n is an integer (18). With this restriction, the number of multiplications decreased and Fourier transformation speed increased.

The first commercial FT hardware was an accessory offered in 1968 for Varian's HA-100 spectrometer. In 1969, Bruker Instruments introduced the first commercial FT-NMR spectrometer, the WH-90, which was a multinuclear spectrometer that ran ^1H NMR at 90 MHz. This was followed in 1970 by the WH-270, the first commercial FT spectrometer using a superconducting magnet. The development of commercial FT-NMR spectrometers enormously increased the application of NMR to chemical problems. With more efficient signal averaging in the time domain, detection limits for ^1H NMR were lowered, and it became practical to measure NMR spectra of less-sensitive and less-abundant nuclei, particularly ^{13}C .

Multiple pulse NMR

With the ability to manipulate the nuclear magnetization by rf pulses, NMR spectroscopists began to devise entirely new experiments based on multiple pulse sequences, such as the inversion-recovery and spin-echo pulse sequences (Figure 3a and b) for measuring spin-lattice (T_1) and spin-spin (T_2) relaxation times for each resonance in multiline NMR spectra (19, 20).

NMR spectroscopists soon realized that these multiple pulse sequences could be used in other ways to increase the range of NMR applications. For example, with the inversion-recovery and spin-echo pulse sequences, spectra can be edited by using T_1 and T_2 as additional resolution parameters. Differences be-

tween the T_1 values of water and solute protons were used to reduce the size of the intense water resonance (often 100,000 or more times as intense as solute resonances) in ^1H NMR spectra of aqueous solutions, whereas differences in T_2 were used to selectively eliminate ^1H resonances of macromolecules in ^1H NMR spectra of mixtures containing proteins and small biological molecules, such as the intracellular region of intact red blood cells (21, 22).

Other problems were addressed with new multiple pulse experiments. Spin-echo methods with gated broadband ^1H decoupling (Figure 3c) were developed for determining the number of attached protons in ^{13}C NMR (the attached proton test [APT] experiment) (23, 24). In the APT spectrum, ^{13}C resonances are singlets, but the relative phase of a resonance depends on the number of attached protons. The APT experiment was followed by the distortionless enhancement by polarization transfer (DEPT) experiment (Figure 3d), which provides similar information but is based on multiple quantum coherence at specific time periods during the pulse sequence (25). The APT and DEPT experiments have replaced off-reso-

nance decoupling for determining the number of attached protons, the first step in the assignment of a ^{13}C spectrum. The insensitive nuclei enhanced by polarization transfer (INEPT) experiment (Figure 3e) transfers the much larger proton polarization to directly bonded, low- γ nuclei, such as ^{13}C or ^{15}N (26). S/N is increased by up to $\gamma_{\text{H}}/\gamma_{\text{C}}$ ($= 4.0$) for ^{13}C and up to $\gamma_{\text{H}}/\gamma_{\text{N}}$ ($= 9.9$) for ^{15}N , which corresponds to a reduction in the signal averaging time by factors up to 16 and 100, respectively.

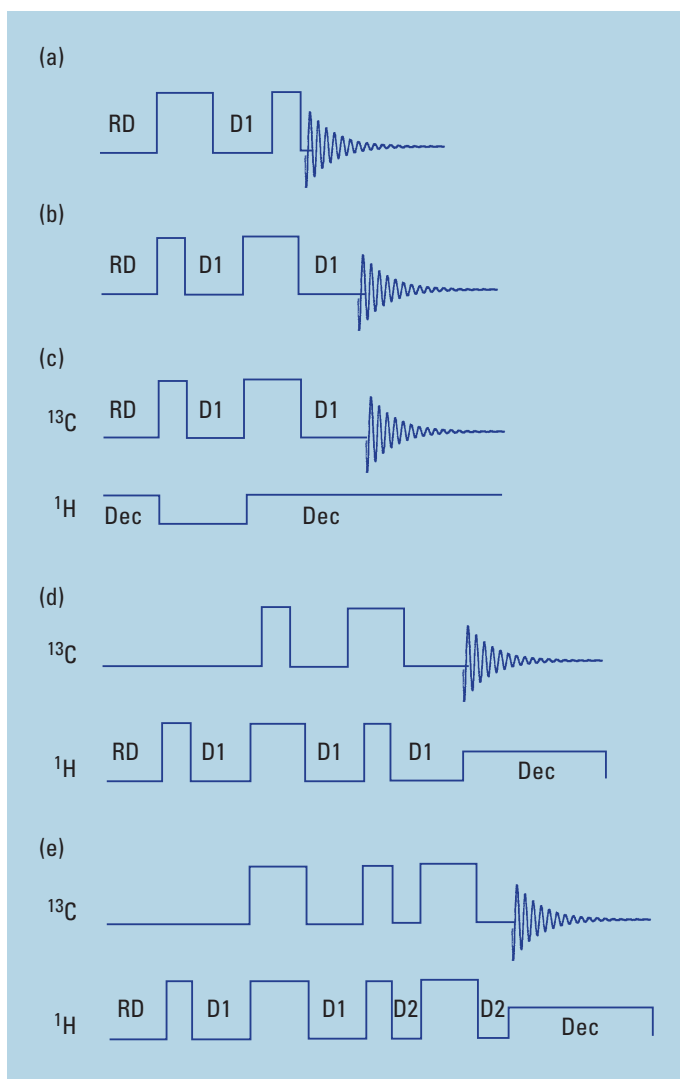
However, the most significant development in multiple pulse NMR was the realization that, by manipulating nuclear spin magnetization with carefully timed rf pulses, dubbed “spin choreography” by Freeman (27), a second frequency dimension could be added to the experiment.

Two-dimensional NMR

Jeener first suggested two-dimensional (2-D) FT-NMR in 1971 (28). Jeener proposed a simple two-pulse sequence—a 90° pulse followed by a time interval (t_1), another 90° pulse, and then acquisition of the FID as a function of time (t_2)—with the collection of a series of FIDs at incremented t_1 values to generate a 2-D data matrix $\mathbf{S}(t_1, t_2)$. He proposed that a double Fourier transformation with respect to t_1 and t_2 would give a 2-D spectrum with two frequency axes, $\mathbf{S}(F_1, F_2)$, and that there would be cross peaks between resonances linked by spin-spin coupling due to transfer of coherence by the second 90° pulse.

FIGURE 3. Pulse sequences for selected 1-D multiple pulse experiments.

The narrow and wide pulses have flip angles of 90° and 180° , respectively. RD represents a relaxation delay during which the magnetization returns to equilibrium between repetitions of the pulse sequence. (a) The inversion-recovery pulse sequence for measuring T_1 and editing spectra on the basis of differences in T_1 s. The macroscopic magnetization is inverted by the 180° pulse and then allowed to relax back toward equilibrium by spin-lattice relaxation during the delay of length D1. The 90° pulse serves as an observation pulse by converting the M_z at time D1 into observable transverse magnetization. (b) The spin-echo pulse sequence for measuring T_2 and editing spectra on the basis of differences in T_2 s. The 90° pulse creates transverse magnetization, which then undergoes spin-spin relaxation for a period of length 2D1. The 180° pulse serves to refocus macroscopic magnetization, which has fanned out during the first D1 interval due to magnetic field inhomogeneity. (c) ^{13}C spin-echo pulse sequence with gated broadband ^1H decoupling (Dec). The broadband decoupling modulates the intensity of the singlet ^{13}C resonances according to the number of attached protons. A similar intensity modulation can be achieved by applying a 180° ^1H pulse simultaneously with the 180° ^{13}C pulse. (d) The DEPT pulse sequence for transfer of polarization from ^1H to ^{13}C and for spectral editing according to the number of attached protons. The 90° ^1H pulse creates ^1H transverse magnetization, which precesses under the influence of ^{13}C , ^1H spin-spin coupling during the first delay of length D1. The 90° ^{13}C pulse then converts the proton magnetization into ^1H , ^{13}C double quantum coherence, which precesses during the second D1 interval. The double quantum coherence is converted to observable single quantum ^{13}C transverse magnetization by the second 90° ^1H pulse. The 180° ^1H and ^{13}C pulses are refocusing pulses, as in the spin-echo pulse sequence. (e) The refocused INEPT pulse sequence for transfer of polarization from ^1H to ^{13}C . The 90° ^1H pulse creates transverse ^1H magnetization, which precesses under the influence of ^{13}C , ^1H spin-spin coupling during the first D1 delay. The first pair of 180° $^1\text{H}/^{13}\text{C}$ pulses results in refocused antiphase ^1H magnetization at the end of the second D1 delay. The simultaneous 90° ^1H and ^{13}C pulses convert the antiphase ^1H magnetization into antiphase ^1H -polarized ^{13}C magnetization, which is allowed to refocus during the two D2 periods. The simultaneous 180° ^1H and ^{13}C pulses, which separate the two D2 delay periods, serve to refocus spin-spin coupling and magnetic field inhomogeneity effects, respectively.



In effect, information about the nuclear spins encoded during the t_1 interval would be determined indirectly by Fourier transformation as a function of both t_1 and t_2 .

In 1975, Müller, Kumar, and Ernst reported the first 2-D NMR spectrum, a 2-D spin, “ \mathcal{F} -resolved” ^{13}C spectrum of hexane, in which proton-coupled ^{13}C multiplets were rotated 90° around their centers so that they were displayed on one frequency axis and the chemical shifts were displayed on the second frequency axis (29). This was followed in 1976 by a seminal publication in which Aue, Bartholdi, and Ernst presented a comprehensive theoretical treatment of 2-D NMR spectroscopy, together with applications, such as correlation, \mathcal{F} -resolved, and multiple quantum spectroscopies (30). Since then, numerous 2-D NMR experiments have been developed by many research groups, including those of Ernst, Freeman, Bax, and Müller. Ernst received the 1991 Nobel Prize in Chemistry for his many contributions to NMR.

The development of 2-D NMR has revolutionized the practice of NMR. 2-D NMR experiments identify resonances that are connected by through-bond scalar coupling, through-space (dipolar) interactions, or chemical exchange. 2-D experiments can be described in terms of four time periods: preparation, evolution (t_1), mixing, and detection (t_2). The preparation period consists of a delay to allow the spin system to relax between repetitions of the pulse sequence, followed by one or more pulses to excite the spin system. During the evolution period, the spin system evolves under the influence of chemical shifts and spin–spin coupling. One or more rf pulses are applied to achieve coherence transfer (by spin–spin coupling) and incoherent transfer (by dipolar interactions or chemical exchange) and to create an observable transverse magnetization, which is detected as a function of t_2 .

In 2-D experiments based on coherence transfer, cross peaks are observed between resonances linked by through-bond spin–spin coupling. They include the homonuclear correlation spectroscopy (COSY) and total correlation spectroscopy (TOCSY) experiments, the incredible natural-abundance double-quantum transfer experiment (INADEQUATE), and the heteronuclear correlation (HETCOR) spectroscopy and heteronuclear multiple quantum coherence (HMQC) experiments.

The COSY experiment, based on the two-pulse sequence originally proposed by Jeener, is one of the simplest and most useful of the 2-D experiments (30). The COSY spectrum consists of peaks along the diagonal that have the same frequency coordinates in both dimensions and correspond to the 1-D spectrum, and off-diagonal cross peaks that identify resonances linked by spin–spin coupling. This same information can be obtained from a series of selective 1-D homonuclear decoupling experiments. However, the COSY experiment provides the complete homonuclear spin–spin coupling network in one

The most significant development was that a second frequency dimension could be added to the experiment.

spectrum with improved resolution, because the spectrum is spread into two dimensions. The TOCSY spectrum also consists of peaks corresponding to the 1-D spectrum along the diagonal, but with cross peaks that can step further along a scalar-coupled spin system (31).

The HETCOR spectrum consists of cross peaks that correlate ^1H resonance frequencies in one dimension with the resonance frequencies of directly bonded heteroatoms, such as ^{13}C , in the second dimension (32). The ^1H , ^{13}C -HETCOR experiment has proven to be extremely useful for assigning ^{13}C spectra, but it suffers from relatively low sensitivity.

In 1979, Müller reported the HMQC experiment, which provides the same ^1H - ^{13}C resonance connectivity information, but has significantly higher sensitivity because the ^1H FID is detected (33). In this experiment, the preparation period consists of a 90° ^1H pulse to excite the proton spin system, which includes protons attached to ^{12}C and ^{13}C , a fixed delay, and then a 90° ^{13}C pulse to create multiple quantum coherence from the ^{13}C nuclei and attached proton(s). Evolution of the multiple quantum coherence cannot be detected directly; rather, it is converted to observable single quantum ^1H coherence by a second 90° ^{13}C pulse and then detected indirectly through its effect on the ^1H FID.

The COSY, TOCSY, HETCOR, and HMQC experiments have greatly simplified the assignment of ^1H and ^{13}C NMR spectra and have made NMR an extremely powerful method for identifying organic compounds. However, the INADEQUATE experiment, which is based on spin–spin coupling between directly bonded pairs of ^{13}C nuclei, is perhaps the ultimate 2-D NMR experiment for determining structural formulae of organic compounds. The carbon backbone of an organic compound can be traced out, one carbon at a time, from cross peaks in the INADEQUATE spectrum (34). Unfortunately, because only 1 in every 10,000 pairs of carbons will both be ^{13}C , the INADEQUATE experiment is of such low sensitivity that it has found limited application. Recent reports suggest that, by using pattern recognition methods, the potential of this experiment may be realized.

In 2-D experiments based on the incoherent transfer of magnetization by the NOE or chemical exchange during the

mixing period, cross peaks are observed between resonances linked by through-space dipole–dipole interactions or by chemical exchange. These experiments include nuclear Overhauser effect spectroscopy (NOESY), rotating frame overhauser effect spectroscopy (ROESY), and exchange spectroscopy (EXSY) (35, 36). The NOE falls off as the inverse sixth power of the distance between the dipoles, and thus cross peaks in NOESY and ROESY spectra provide information about the conformation and structure of molecules in solution. To illustrate, a portion of the ROESY spectrum of a 19-amino acid peptide is shown in Figure 4 (37).

In 1985, Wüthrich and co-workers reported the complete 3-D structure of a protein in solution using only NOE distance constraints (38). Since then, there has been spectacular progress in developing and applying NMR methodology to protein structure determination. NMR and X-ray crystallography can determine the 3-D structures of proteins. However, only NMR can determine the structures of proteins in solution.

Multidimensional NMR

Because of resonance overlap, protein structure determination by 2-D NMR was limited to relatively small proteins. A major milestone in protein NMR was the development of 3-D and 4-D NMR along with methods for producing uniformly ^{15}N - and ^{13}C -labeled proteins (39, 40). 3-D and 4-D NMR experiments link two or three of the 2-D experiments just described. Together, they produce a multidimensional data matrix, which, when Fourier transformed, produces a 3-D or 4-D spectrum. The third dimension can be used, for example, to spread apart an ^1H , ^1H -2-D spectrum on the basis of the chemical shift of another nucleus, such as ^{15}N or ^{13}C . For instance, an ^1H , ^1H -TOCSY spectrum of a uniformly ^{15}N -labeled peptide or protein can be spread apart according to the chemical shift of the backbone amide ^{15}N resonance for each amino acid using a 3-D HMQC-TOCSY experiment. With the resolution that can be achieved with these multidimensional experiments, it has been possible to extend the NMR method for determining protein structure to larger and larger proteins.

NMR theory

As NMR evolved from the cw to FT-NMR to multidimensional NMR, the theory also evolved, providing a basis for designing experiments based on such esoteric concepts as the indirect detection of multiple quantum coherence and the transfer of coherence from ^1H to ^{15}N to ^{13}C and then back to ^1H in multidimensional experiments with uniformly ^{13}C , ^{15}N -labeled proteins.

Early in the history of NMR, the behavior of nuclear spins in a magnetic field was treated using classical mechanics. By considering the macroscopic, measurable magnetization of an ensemble of nuclei (Figure 2), Bloch formed a set of equations to describe the magnetic resonance phenomenon in terms of a classical vector model (41). This vector model has served admirably to explain several aspects of NMR, including T_1 and T_2 relaxation and the behavior of the macroscopic magnetization during various multiple pulse experiments. A major virtue of the vector model is that it helps visualize NMR experiments in

terms of a simple physical picture. A limitation, however, is that only the simplest of the 2-D experiments can be adequately described.

2-D experiments based on coherence transfer and multiple quantum coherence can be described in terms of a density matrix treatment, which provides a complete description of the state of the spin system and its time evolution during a pulse sequence (42). However, the density matrix treatment becomes quite cumbersome for systems with a large number of spins and provides little insight into the experiment. The product operator formalism, which is derived from the density matrix treatment, offers a simpler but more complete theoretical treatment of the behavior of weakly coupled spin systems during a pulse sequence, while also providing a physical pictorial interpretation somewhat analogous to the vector model (43). The product operator formalism has played a key role in the design of multidimensional NMR experiments.

NMR and the periodic table

Most elements have at least one stable, NMR-active isotope. For sensitivity reasons, most cw NMR measurements were made on ^1H , ^{19}F , and ^{31}P . With the development of FT-NMR, high-field spectrometers, and polarization transfer and indirect detection experiments, it is now possible to routinely obtain NMR spectra of ^{13}C , ^{15}N , and other low-abundance, low- γ isotopes. The extent to which specific isotopes have been studied has been a function of their nuclear spin properties (favoring $I = 1/2$ nuclei over $I > 1/2$), γ , and the level of chemical interest in the element. Nuclei with $I = 1/2$ have relatively long relaxation times, which results in narrow resonance lines suitable for high-resolution NMR studies. Twenty-four elements have stable isotopes with $I = 1/2$, including ^{13}C . Because of ^{13}C NMR's usefulness in elucidating the structures of organic molecules, it has seen explosive growth following the development of FT-NMR.

Nuclei with $I > 1/2$ possess nuclear electric quadrupole moments that shorten relaxation times and broaden resonance lines, making them less suitable for high-resolution studies. However, relaxation times of these nuclei are extremely sensitive to the chemical environment, forming the basis of studies of alkali, alkaline earth, and halide ion binding by biological macromolecules and ion solvation.

NMR of solids

Chemical shifts and spin–spin couplings are usually obscured in NMR spectra of solids by resonance broadening due to dipole–dipole interactions between nearby nuclei and chemical shift anisotropy effects. However, NMR spectroscopists have devised techniques for controlling these interactions so that resonance line widths can be reduced from several kHz to several Hz. These techniques have revolutionized solid-state NMR.

The first breakthrough was the discovery by Andrew in 1958 that broadening due to dipolar interactions can be eliminated by spinning the sample around an axis at the “magic angle” of $54^\circ 44'$ to \mathbf{B}_0 (44). In the magic angle spinning (MAS)

experiment, the sample is contained in a small capsule (rotor) with a length of ~10 mm and a diam of 4–7 mm, which is rotated at speeds of up to 35 kHz. MAS also eliminates broadening due to chemical shift anisotropy.

A second major breakthrough occurred in 1972 when Pines, Gibby, and Waugh reported the use of cross-polarization (CP) to increase the sensitivity of natural abundance ^{13}C NMR spectra of solids (45). In the CP experiment, a double irradiation pulse sequence removes dipolar interactions between isotopically dilute ^{13}C and the much more abundant protons. Polarization is also transferred from the protons to the dilute ^{13}C spins (CP) to increase population differences between adjacent ^{13}C energy levels. The result is an increase in ^{13}C resonance intensities by a factor of $\gamma_{\text{H}}/\gamma_{\text{C}}$.

In 1976, Schaefer and Stejskal reported the combined CP-MAS experiment, which has become the standard method for measuring high-resolution NMR spectra of ^{13}C , ^{15}N , and other low-sensitivity, low-abundance $I = 1/2$ nuclei in the solid state (46). High-resolution ^{13}C NMR spectra are routinely measured for microcrystalline materials, crystal powders, and amorphous materials by CP-MAS NMR. It is interesting to note that, although line-narrowing by MAS was first reported in 1958, it was not until almost 20 years later that it was used routinely for solid-state NMR.

NMR instrumentation

Magnets. Ever since the first commercial NMR spectrometer was introduced, there has been a continuous effort to increase the field strengths of NMR magnets. Sensitivity increases in proportion to $\mathbf{B}_0^{3/2}$, chemical shift dispersion increases linearly with \mathbf{B}_0 , and spectral interpretation is simplified as \mathbf{B}_0 is increased.

Commercial spectrometers during the 1950s and early 1960s were based on permanent magnets and electromagnets. \mathbf{B}_0 was limited to 2.11 T (90-MHz ^1H NMR) with permanent magnets and 2.35 T (100-MHz ^1H NMR) with electromagnets.

The development of persistent superconducting solenoids for use in NMR magnets (cryomagnets) in the early 1960s was a major milestone. Superconducting solenoids carry much higher current densities, making it possible to achieve higher magnetic fields. The current state-of-the-art field strength is 18.8 T (800-MHz ^1H NMR), with the first 900-MHz (21.1-T) spectrometers scheduled for delivery this year.

NMR magnets must meet two very demanding criteria: \mathbf{B}_0 must be both stable and homogenous over the volume detected by the receiver coil. For example, resonance lines might be as narrow as 0.1 Hz at half height for very high-resolution applications, corresponding to 1 part in 5 billion for ^1H NMR at 500 MHz. \mathbf{B}_0 stability is achieved with a field/frequency lock that provides a feedback signal to correct for drift—an innovation introduced in the 1950s to correct for the instability of electromagnets. \mathbf{B}_0 homogeneity is achieved with current shims, which produce local \mathbf{B}_0 gradients to compensate for inhomogeneities in the static magnetic field, and by spinning the sample, which averages \mathbf{B}_0 inhomogeneity transverse to the spinning axis. With the high-quality superconducting magnets now

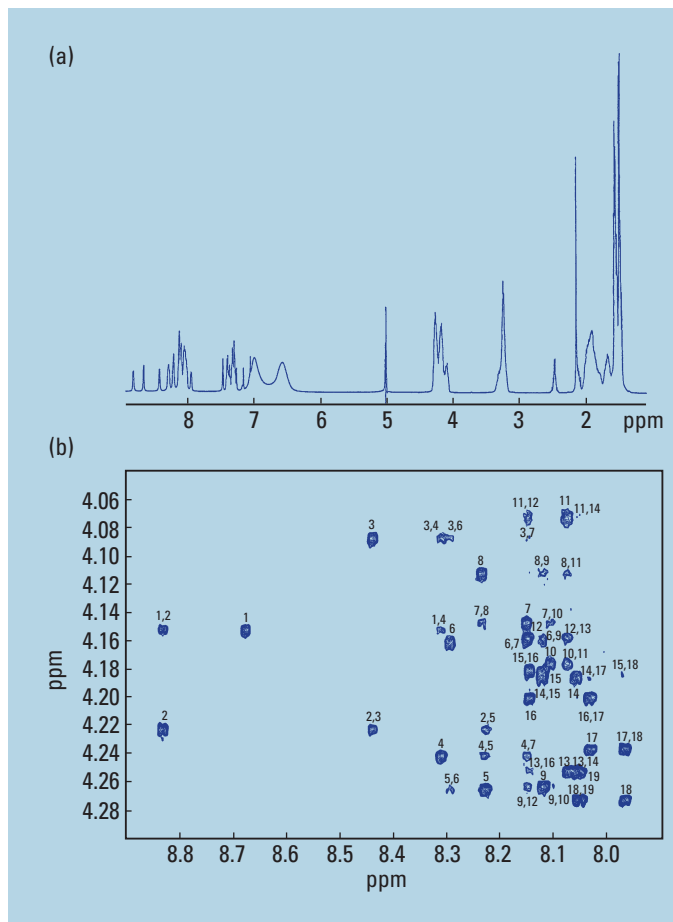


FIGURE 4. (a) The 500-MHz 1-D ^1H NMR spectrum and (b) a portion of the 2-D ROESY spectrum for a 19-amino acid peptide.

Peptide is N-Ac-Ala-Glu-Ala-Ala-Ala-Arg-Ala-Ala-Ala-Arg-Arg-Ala-Ala-Arg-Arg-Ala-Ala-Ala-Arg-NH₂, which is in 90% H₂O/10% D₂O. The H₂O resonance at ~5.0 ppm was suppressed by presaturation. The ROESY spectrum was measured using the band-selective homonuclear decoupled (BASHD) ROESY pulse sequence (38), which collapses multiplets due to ^1H , ^1H spin-spin coupling to singlets in the F1 dimension to further increase resolution in the 2-D spectrum. The C $_{\alpha}$ H (4.04–4.30 ppm)/amide NH (7.9–8.9 ppm) region of the BASHD-ROESY spectrum is shown. Because there are 12 Ala and 6 Arg residues in the peptide, there is extensive overlap in the 1-D spectrum, particularly in the C $_{\alpha}$ H region. However, cross peaks for all of the possible NH $_i$ -C $_{\alpha}$ H $_j$ and C $_{\alpha}$ H $_i$ -NH $_{i+1}$ dipolar interactions are observed in the BASHD-ROESY spectrum, making it possible to completely assign the ^1H NMR spectrum of the peptide. The cross peaks for intra-residue NH $_i$ -C $_{\alpha}$ H $_i$ and inter-residue C $_{\alpha}$ H $_i$ -NH $_{i+1}$ dipolar interactions are identified by single numbers and pairs of consecutive numbers, respectively, which indicate amino acid residues starting from the N-terminal Ala. Additionally, cross peaks for NH $_i$ -C $_{\alpha}$ H $_{i+3}$ dipolar interactions are also observed, which indicate the peptide is an α -helix in solution. (Adapted with permission from Ref. 37)

in use, it often is not necessary to spin the sample to achieve superb \mathbf{B}_0 homogeneity.

The need for increased sensitivity and chemical shift dispersion has been the driving force for increasing magnet strength. If these were the only gains, it might be difficult to justify the substantial price increases for the relatively small gains in sensitivity and dispersion when going from 700 to 800 MHz or 800 to 900 MHz, for example. However, these very high field

Many NMR phenomena have been discovered, and powerful experiments have been devised for observing them.

strengths provide other significant benefits, particularly for NMR of biological macromolecules.

For example, determination of protein 3-D structures by NMR was limited to proteins of molecular weights $< \sim 20\text{--}30$ kDa, because resonances become broader with increasing protein size. Recently, however, Wüthrich and co-workers discovered that, at the very high magnetic field strengths, narrow resonances can be obtained by the constructive use of interference between dipole-dipole coupling and chemical shift anisotropy in a technique called *transverse relaxation-optimized spectroscopy* (TROSY) (47). With TROSY experiments, it should be possible to determine 3-D structures of proteins ≥ 100 kDa.

Probe. The sample is inserted into the probehead, which contains the transmitter and receiver coil(s). Probes have been developed to accommodate a range of sample sizes. The standard is a sample volume of 400–700 μL in a 5-mm o.d. NMR tube. To increase the sensitivity for low abundance, low- γ nuclei probes have been designed to accommodate 10-, 15-, and even 30-mm o.d. NMR tubes.

More recently, there has been an emphasis on measuring spectra of very small quantities, particularly using ^1H NMR spectra. Probes have been designed with smaller rf coils for microliter and nanoliter sample volumes (47, 48), and MAS probes have been built for measuring high-resolution NMR spectra with sample volumes of tens of microliters (49). Signal broadening due to magnetic susceptibility discontinuities across the region sampled by the receiver coil can be eliminated by rotating the sample at high speeds around an axis at the magic angle. MAS probes have also proven useful for measuring high-resolution NMR spectra of samples not amenable to standard liquid-phase methods, such as peptides and other compounds on solid-phase synthesis resins (50).

The use of cryogenically cooled receiver coils in NMR probes is particularly interesting, because the noise voltage associated with signal detection is reduced. This recent development holds the promise of significantly lower detection limits (51).

Pulsed-field gradients. First described in 1980 as an alternative method for selecting the desired coherences in 2-D

NMR, pulsed-field gradients (PFGs) were incorporated into high-resolution NMR instrumentation about a decade later (52, 53).

Linear magnetic field gradients of short duration are applied over the sample volume (e.g., along the z axis) at specific times during a multiple pulse sequence. The gradient will dephase coherences spatially, along the direction of the gradient; the extent of dephasing depends on the coherence (e.g., single quantum vs double quantum). By using the appropriate combination of rf pulses and PFGs, the desired coherences can be selectively rephased and detected. Because the receiver

detects only the desired coherence, its gain can be set much higher, making possible multidimensional experiments in a fraction of the time required for phase cycling experiments.

PFGs are also the basis of methods for eliminating the water resonance from ^1H NMR spectra of aqueous solutions and measuring diffusion coefficients. In an experiment that will have many applications, differences in diffusion coefficients are used as the basis for spectral editing (54).

Computers. The importance of the computer revolution to the development of modern NMR spectroscopy cannot be overstated. Indeed, the development of FT-NMR as a practical alternative to cw NMR had to await the arrival of minicomputers. The FT accessory for the HA-100 had a minicomputer with only 4000 bytes of memory, which severely limited digital resolution in the frequency domain spectrum.

Advances in computer technology have been rapidly incorporated into NMR spectrometers. Today, the user shims the magnet to optimize \mathbf{B}_0 homogeneity usually automatically with an algorithm that uses PFGs, selects the pulse sequence, sets the timing and pulse parameters for the pulse programmer, controls the sample temperature, and initiates the experiment through the computer interface. Digitized data are then processed, and the spectra are displayed by the computer. With the computing speed and large memory of today's workstations, a 2-D data set consisting of, for example, 512 8K FIDs can be processed in minutes.

Mature—not dormant

NMR spectroscopists recently celebrated the 50th anniversary of the first NMR observations in condensed phases. Today, NMR is one of chemistry's most important spectroscopic techniques. Numerous NMR phenomena have been discovered, and powerful experimental methods have been devised for observing them. NMR is the preeminent method for determining the structure of organic compounds. NMR is also widely used to determine the structures and characterize the solution chemistry of inorganic and organometallic compounds (55). NOE data, together with spin-spin-coupling constants, provide a sensitive probe of the conformations of molecules and form the basis of NMR methods for determining the 3-D

structures of proteins and other biological macromolecules in solution (56).

NMR is widely used for studying chemical equilibria and kinetics at the molecular level. For example, acid dissociation constants have been determined for specific acidic groups in peptides and proteins using chemical shift data, and NMR line broadening and magnetization transfer methods are widely used to characterize the kinetics of intramolecular and intermolecular reactions at equilibrium (57).

NMR offers important advantages as a technique for quantitative chemical analysis, including its nondestructive nature, easy analysis of multicomponent mixtures, and no need to calibrate the instrument with pure samples of each analyte (58). Recently, NMR has emerged as an information-rich detector in LC/NMR—a combination that is particularly promising for the pharmaceutical industry (59).

Although NMR is a mature technique, it certainly is not dormant. New developments in methodology and instrumentation continue at a rapid pace, and scientists from a range of disciplines continue to find new applications. To illustrate, the neural patterns in the human brain associated with pain, the anticipation of pain, and fear have recently been identified by functional magnetic resonance imaging (60).

Dallas L. Rabenstein is a professor of chemistry at the University of California—Riverside. His research interests include NMR spectroscopy and its application in characterizing peptides, proteins, carbohydrates, biological fluids, and intact red blood cells. Correspondence about this article should be addressed to Rabenstein at the Department of Chemistry, University of California, Riverside, CA 92521 (dlrab@ucr.ac1.ucr.edu).

References

- (1) Pauli, W. *Naturwissenschaften* **1924**, *12*, 741.
- (2) Gerlach, W.; Stern, O. *Ann. Phys. (Leipzig)* **1924**, *74*, 673.
- (3) Rabi, I. I.; Zacharias, J. R.; Millman, S.; Kusch, P. *Phys. Rev.* **1938**, *53*, 318.
- (4) Bloch, F.; Hansen, W. W.; Packard, M. E. *Phys. Rev.* **1946**, *69*, 127.
- (5) Purcell, E. M.; Torrey, H. C.; Pound, R. V. *Phys. Rev.* **1946**, *69*, 37.
- (6) Proctor, W. G.; Yu, F. C. *Phys. Rev.* **1950**, *77*, 717.
- (7) Dickinson, W. C. *Phys. Rev.* **1950**, *77*, 736.
- (8) Arnold, J. T.; Dharmatti, S. S.; Packard, M. E. *J. Chem. Phys.* **1951**, *19*, 507.
- (9) Meyer, L. H.; Saika, A.; Gutowsky, H. S. *J. Am. Chem. Soc.* **1953**, *75*, 4567.
- (10) Proctor, W. G.; Yu, F. C. *Phys. Rev.* **1951**, *81*, 20.
- (11) Gutowsky, H. S.; McCall, D. W. *Phys. Rev.* **1951**, *748*, 82.
- (12) Hahn, E. L.; Maxwell, D. E. *Phys. Rev.* **1951**, *84*, 1246.
- (13) Purcell, E. M.; Ramsey, N. F. *Phys. Rev.* **1952**, *85*, 142.
- (14) Shoolery, J. N. *Anal. Chem.* **1933**, *65*, 731 A.
- (15) Ernst, R. R.; Anderson, W. A. *Rev. Sci. Instrum.* **1966**, *37*, 93.
- (16) Hahn, E. L. *Phys. Rev.* **1950**, *80*, 580.
- (17) Freeman, R. *Anal. Chem.* **1933**, *65*, 743 A.
- (18) Cooley, J. W.; Tukey, J. W. *Mathematical Computation* **1965**, *19*, 297.
- (19) Vold, R. L.; Waugh, J. S.; Klein, M. P.; Phelps, D. E. *J. Chem. Phys.* **1968**, *43*, 3831.
- (20) Freeman, R.; Hill, H. D. W. In *Dynamic Nuclear Magnetic Resonance Spectroscopy*; Jackman, L. M., Cotton, F. A., Eds.; Academic Press: New York, 1975; p 131.
- (21) Patt, S. L.; Sykes, B. D. *J. Chem. Phys.* **1972**, *56*, 3182.
- (22) Brown, F. F.; Campbell, I. D.; Kuchel, P. W.; Rabenstein, D. L. *FEBS Lett.* **1977**, *82*, 12.
- (23) Rabenstein, D. L.; Nakashima, T. T. *Anal. Chem.* **1979**, *51*, 1465 A.
- (24) Patt, S.; Shoolery, J. N. *J. Magn. Reson.* **1982**, *46*, 535.
- (25) Bendall, M. R.; Doddrell, D. M.; Pegg, D. T. *J. Am. Chem. Soc.* **1981**, *103*, 4603.
- (26) Morris, G. A.; Freeman, R. *J. Am. Chem. Soc.* **1979**, *101*, 760.
- (27) Freeman, R. *Spin Choreography*; Oxford University Press: Oxford, U.K., 1998.
- (28) Jeener, J. In *Encyclopedia of Nuclear Magnetic Resonance*; Grant, D. M., Harris, R. K., Eds.; John Wiley and Sons: Chichester, England, 1996; Vol. 1, p 409.
- (29) Müller, L.; Kumar, A.; Ernst, R. R. *J. Chem. Phys.* **1975**, *63*, 5490.
- (30) Aue, W. P.; Bartholdi, E.; Ernst, R. R. *J. Chem. Phys.* **1976**, *64*, 2229.
- (31) Bax, A.; Davis, D. G. *J. Magn. Reson.* **1985**, *65*, 355.
- (32) Freeman, R.; Morris, G. A. *J. Chem. Soc., Chem. Commun.* **1978**, 684.
- (33) Müller, L. *J. Am. Chem. Soc.* **1979**, *101*, 4481.
- (34) Bax, A.; Freeman, R.; Frenkiel, T. A. *J. Am. Chem. Soc.* **1981**, *103*, 2102.
- (35) Jeener, J.; Meier, B. H.; Bachmann, P.; Ernst, R. R. *J. Chem. Phys.* **1979**, *71*, 4546.
- (36) Bothner-By, A. A.; Stephens, R. L.; Lee, J.-M.; Warren, C. D.; Jeanloz, R. W. *J. Am. Chem. Soc.* **1984**, *106*, 811.
- (37) Kaerner, A.; Rabenstein, D. L. *Magn. Reson. Chem.* **1998**, *36*, 601.
- (38) Williamson, M. P.; Havel, T.; Wüthrich, K. *J. Mol. Biol.* **1985**, *182*, 295.
- (39) Fesik, S. W.; Gampe, R. T.; Zuiderweg, E. R. P. *J. Am. Chem. Soc.* **1989**, *111*, 770.
- (40) Griesinger, C.; Sørensen, O. W.; Ernst, R. R. *J. Magn. Reson.* **1989**, *84*, 14.
- (41) Bloch, F. *Phys. Rev.* **1946**, *70*, 460.
- (42) Ernst, R. R.; Bodenhausen, G.; Wokaun, A. *Principles of Nuclear Magnetic Resonance in One and Two Dimensions*; Oxford University Press: Oxford, U.K., 1987.
- (43) Sørensen, O. W.; Eich, G. W.; Levitt, M. H.; Bodenhausen, G.; Ernst, R. R. *Prog. Nucl. Magn. Reson. Spectrosc.* **1983**, *16*, 163.
- (44) Andrew, E. R.; Bradbury, A.; Eades, R. G. *Nature* **1958**, *182*, 1659.
- (45) Pines, A.; Gibby, M. G.; Waugh, J. S. *J. Chem. Phys.* **1972**, *56*, 1756.
- (46) Schaefer, J.; Stejskal, E. O. *J. Am. Chem. Soc.* **1976**, *98*, 1031.
- (47) Pervushin, K.; Riek, R.; Wider, G.; Wüthrich, K. *Proc. Natl. Acad. Sci. U.S.A.* **1997**, *94*, 12366.
- (48) Olson, D. L.; Lacey, M. E.; Webb, A. G.; Sweedler, J. V. *Anal. Chem.* **1999**, *71*, 3070.
- (49) Shoolery, J. N. *Prog. Nucl. Magn. Reson. Spectrosc.* **1995**, *28*, 37.
- (50) Keifer, P. A.; Baltusis, L.; Rice, D. M.; Tymiak, A. A.; Shoolery, J. N. *J. Magn. Reson., Ser. A* **1996**, *119*, 65.
- (51) Flynn, P. F.; Mattiello, D. L.; Hill, H. D. W.; Wand, A. J. *J. Am. Chem. Soc.* **2000**, *122*, 4823.
- (52) Bax, A.; De Jong, P. G.; Mehlkopf, A. F.; Schmidt, J. *Chem. Phys. Lett.* **1980**, *69*, 567.
- (53) Hurd, R. E. *J. Magn. Reson.* **1990**, *87*, 422.
- (54) Dixon, A. M.; Larive, C. K. *Appl. Spectrosc.* **1999**, *53*, 426A.
- (55) Akitt, J. W.; Mann, B. E. *NMR and Chemistry*; Stanley Thornes Publishers: Cheltenham, U.K., 2000.
- (56) Wüthrich, K. *NMR of Proteins and Nucleic Acids*; Wiley-Interscience: New York, 1986.
- (57) Evans, J. N. S. *Biomolecular NMR Spectroscopy*; Oxford University Press: Oxford, U.K., 1995.
- (58) Rabenstein, D. L.; Keire, D. A. In *Modern NMR Techniques and Their Applications in Chemistry*; Popov, A. I., Hallenga, K., Eds.; Marcel Dekker: New York, 1990; p 323.
- (59) Albert, K. *J. Chromatogr., A* **1999**, *856*, 199.
- (60) Ploghaus, A., et al. *Science* **1999**, *284*, 197.